

Hybrid Model-Based and Data-Driven Wind Velocity Estimator for the Navigation System of a Robotic Airship

Apolo Silva Marton · André Ricardo Fioravanti · José Raul Azinheira · Ely Carneiro de Paiva

Abstract In the context of autonomous airships, several works in control and guidance use wind velocity to design a control law. However, in general, this information is not directly measured in robotic airships. This paper presents three alternative versions for estimation of wind velocity. Firstly, an Extended Kalman Filter is designed as a model-based approach. Then a Neural Network is designed as a data-driven approach. Finally, a hybrid estimator is proposed by performing a fusion between the previous designed estimators: model-based and data-driven. All approaches consider only GPS, IMU and Pitot tube as available sensors. Simulations in a realistic nonlinear model of the airship suggest that the cooperation between these two techniques increases the estimation performance.

Keywords Wind estimation, Extended Kalman Filter, Neural Network, Robotic Airship

A. S. Marton
Department of Computational Mechanics, School of Mechanical Engineering, Mendeleev Street, 200, 13083-180, University of Campinas, Brazil
E-mail: apolosm@fem.unicamp.br

A. R. Fioravanti
Department of Computational Mechanics, School of Mechanical Engineering, Mendeleev Street, 200, 13083-180, University of Campinas, Brazil
E-mail: fioravanti@fem.unicamp.br

J. R. Azinheira
Department of Mechanical Engineering, Instituto Superior Técnico, Lisbon, 1049-001, Portugal
E-mail: jose.raul.azinheira@tecnico.ulisboa.pt

E. C. de Paiva
Department of Integrated Systems, School of Mechanical Engineering, Mendeleev Street, 200, 13083-180, University of Campinas, Brazil
E-mail: elyapaiva@fem.unicamp.br

1 Introduction

Recently, Unmanned Aerial Vehicles (UAVs) become useful in several applications due to their economic efficiency and mobility. For outdoor applications, air related information such as: angle of attack, sideslip and wind velocity, helps to improve the control performance.

Outdoor airships commonly have a guidance control to track a trajectory. The first idea is that the attitude reference shall be coincident with the reference trajectory attitude. However, there are two situations when this is not desirable: in the presence of wind disturbances (an almost certainty when flying outdoors) and if the objective is ground-hover (since the desired attitude is arbitrarily defined).

An aircraft of conventional shape must fly against the apparent wind in order to have low drag. This is also true for airships, specially because of the lateral underactuation [6]. Therefore, whenever there is wind, the airship must try to align itself with the relative airspeed, thus reducing the sideslip angle. This implies that guidance control also depends on information about wind velocity and attitude. However, measuring such elements is not a trivial task.

The most common solution is to estimate the wind velocity in order to extract the necessary information about the vehicle motion. The Model-based techniques are the most popular strategies. As an example, in [7], it is proposed an approach for estimate the angle of attack and sideslip angle by the kinematic equations of motion of an aerobatic UAV. Meanwhile, with the same kinematic equations, in [3] an Extended Kalman Filter (EKF) is proposed for estimating the wind heading and velocity using an aircraft with a single GPS and Pitot tube. In [5] a wind velocity observer also based in the kinematics is proposed for small UAVs with experimental results. Similarly, in [11] is also proposed an

EKF for wind velocity estimation, however applied to a Stationary stratospheric airship in simulation environment. Then in [8] are presented four Model-based solutions considering an aircraft with four different possible configurations of sensors.

Recently, the Machine Learning approach has become popular in the field of robotics. The impressive growing of computational resources and increasing acquired data over the years have increased the potential of these Data-driven techniques. These strategies were already introduced in applications such as control of aircraft [2] and air data estimation for a Micro-UAV [10]. The wind estimation problem is addressed in [1] using a quadrotor and with a Machine-learning approach. However, a Data-driven online estimation of wind velocity for robotic airships is still a challenge.

This paper presents an alternative version of a Model-based wind velocity estimator using the EKF technique similar to the solution presented in [3], however taking an airship as a case study. Then, a Data-driven approach of estimation using a Neural Network (NN) is proposed. Finally, a hybrid version that uses both Model-based and Data driven techniques is considered. The main tool to validate the proposed solutions is a realistic nonlinear model in Simulink/MATLAB developed since the AURORA project [4] and improved by [6].

This paper is organized as follows: the airship nonlinear modeling is summarized in Sect. 2; then the kinematic equations of motion are analyzed in Sect. 3; an EKF is designed for wind velocity estimation in Sect. 4; the NN approach of wind velocity estimation is presented in Sect. 5; the hybrid version of wind velocity estimation is presented in Sect. 6; the training method used for the Neural Network is described in Sect. 7; validating simulations take place in Sect. 8 by establishing a comparison between the proposed approaches and the approach presented by [3]; finally some conclusions are drawn in Sect. 9.

2 Airship modelling

This work is placed in the context of the DRONI project [9]. The project aims to develop an Unmanned Autonomous Airship to perform monitoring and surveillance missions in the Amazon rainforest. The airship is composed by a hull with 11m length and 2.48m diameter equipped with: 4 vectored propellers with independent thrusters (see Figure 1) and tail surfaces (rudder, elevator and aileron).

This section presents a summary of the mathematical modeling of an airship. For a detailed description,



Fig. 1 Robotic airship performing its first flight.

please refer to [6]. The airship nonlinear model can be expressed as a state-space model given by:

$$\dot{\boldsymbol{\xi}} = g(\boldsymbol{\xi}, \mathbf{x}, \mathbf{d}), \quad (1a)$$

$$\dot{\mathbf{x}} = f(\mathbf{x}, \mathbf{u}, \mathbf{d}), \quad (1b)$$

where:

- the kinematic states $\boldsymbol{\xi} = [\mathbf{P}_{NED}^T \ \boldsymbol{\Phi}^T]^T$ include the cartesian positions $\mathbf{P}_{NED} = [P_N \ P_E \ P_D]^T$ and angular position $\boldsymbol{\Phi} = [\phi \ \theta \ \psi]^T$ in the North-East-Down frame;
- the dynamic states $\mathbf{x} = [\mathbf{V}_g^T \ \boldsymbol{\Omega}^T]^T$ include the linear speed $\mathbf{V}_g = [u \ v \ w]^T$ and angular speed $\boldsymbol{\Omega} = [p \ q \ r]^T$ in the body frame;
- the input vector $\mathbf{u} = [\delta_e \ \delta_a \ \delta_r \ \delta_0 \ \mu_0]^T$ includes: δ_e, δ_a and δ_r which are elevator, aileron and rudder deflection (rad); δ_0 as the normalized thrusters voltage (V/V); μ_0 as the common vectoring angle of the thrusters (rad);
- and, finally, the disturbance vector \mathbf{d} that includes wind velocities and gust parameters.

The dynamics are based on the Newton-Euler equations including five components of forces and moments, namely: F_d containing the Coriolis and centrifugal force terms, and also the wind-induced forces and moments; F_a given by aerodynamic forces and moments; F_p given by propulsion forces and moments; F_g given by gravity forces and moments, which are function of the difference between the weight and buoyancy forces; and F_w given by the wind forces and moments. Therefore, the linear and angular accelerations are given by:

$$f(\mathbf{x}, \mathbf{u}, \mathbf{d}) = \mathbf{M}^{-1} \left(\mathbf{F}_d + \mathbf{F}_a + \mathbf{F}_p + \mathbf{F}_g + \mathbf{F}_w \right), \quad (2)$$

where \mathbf{M} includes mass and inertial coefficients of the airship. These equations are referenced in the body frame centered in the Center of Buoyancy (CB) that is approximately equivalent to the Center of Volume (CV) as shown in Figure 2. The linear and angular positions are updated through kinematic equations (1a).

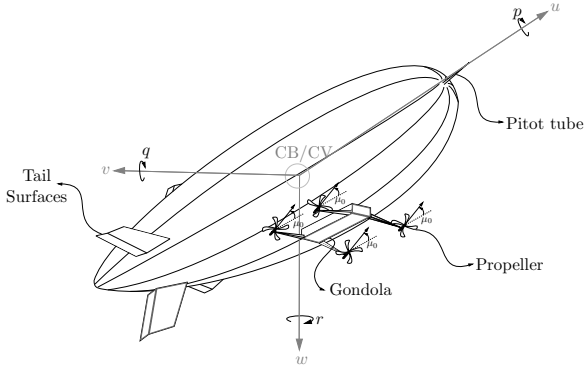


Fig. 2 DRONI airship body diagram.

3 Kinematic Equations of motion

When the displaced fluid mass is not negligible, as is the case for airships, the equations of motion are usually derived using the Lagrangian approach [6]. Let the airship motion be represented by its inertial velocity \mathbf{V}_g . Similarly, the wind is described by an inertial velocity \mathbf{V}_w . The airship relative air velocity is called airspeed (\mathbf{V}_a) and it is given by:

$$\mathbf{V}_a = \mathbf{V}_g - \mathbf{V}_w, \quad (3)$$

where $\mathbf{V}_w = [u_w \ v_w \ w_w]^T$ and $\mathbf{V}_a = [u_a \ v_a \ w_a]^T$.

The Euclidean norm of the airspeed is called *true airspeed* (V_t) and it is given by:

$$V_t = \|\mathbf{V}_a\|_2 = \sqrt{u_a^2 + v_a^2 + w_a^2}. \quad (4)$$

Other important definitions are the sideslip angle β and angle of attack α . The sideslip angle is a relative orientation between the vertical plane of the vehicle and the vector \mathbf{V}_a . Moreover, the angle of attack α is given by the angle between the vector \mathbf{V}_a and the horizontal plane of the vehicle, as shown in Figure 3.

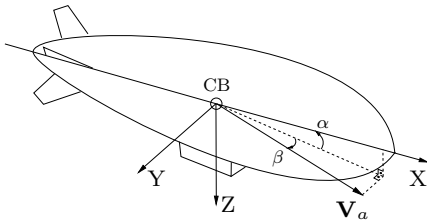


Fig. 3 Sideslip angle (β) and angle of attack (α).

Therefore, we can define β and α by the following statements:

$$\beta = \sin^{-1} \frac{v_a}{V_t}, \quad (5)$$

$$\alpha = \tan^{-1} \frac{w_a}{u_a}. \quad (6)$$

Thus, an equivalent formula is given by:

$$w_a = u_a \frac{\sin \alpha}{\cos \alpha} \quad \text{and} \quad v_a = V_t \sin \beta. \quad (7)$$

Finally, we obtain:

$$V_t = \frac{u_a}{\cos \alpha \cos \beta}. \quad (8)$$

The Pitot tube measures the longitudinal dynamic pressure ΔP in the body frame. Also, it has a correlation with the airspeed as shown below:

$$\Delta P = \eta (u_a)^2, \quad (9)$$

where η is the calibrating factor that is correlated with the air density and pitot efficiency. Since there are uncertainties in the coefficient η , consider the following variable transformation:

$$\Delta P = V_{pitot}^2, \quad (10)$$

Thus, V_{pitot} is correlated with the true airspeed as the following statement:

$$V_t = \frac{V_{pitot}}{\sqrt{\eta} \cos \alpha \cos \beta}, \quad (11)$$

Because there are uncertainties in η and the angles α and β are unmeasurable, those values will be estimated together as another scale factor c_f given by:

$$c_f = \sqrt{\eta} \cos \alpha \cos \beta, \quad (12)$$

therefore (11) becomes:

$$V_t = \frac{1}{c_f} V_{pitot}. \quad (13)$$

Now, consider that the rotation of vector \mathbf{V}_g from the body frame to the NED frame is given by $\mathbf{V}_{NED} = [V_N \ V_E \ V_D]^T$. Also, consider that such rotation applied to vector \mathbf{V}_w is given by \mathbf{V}_{NEDw} . Thus, the airspeed in NED frame is given by:

$$\mathbf{V}_{NEDa} = \mathbf{V}_{NED} - \mathbf{V}_{NEDw} = S(\Phi)^T \mathbf{V}_a. \quad (14)$$

It is known that a rotational operation does not change the vector module, thus the following statement is valid, considering the wind strictly horizontal:

$$V_{pitot}^2 = c_f^2 ((V_N - V_{Nw})^2 + (V_E - V_{Ew})^2 + (V_D)^2). \quad (15)$$

Supposing that, the airship starts from an initial condition where α and β are negligible ($\alpha \approx \beta \approx 0$) we have $u_a = V_t$ and $v_a = w_a = 0$. Therefore in the global frame we have:

$$V_{Na} = u_a \cos \psi \cos \theta, \quad (16)$$

$$V_{E_a} = u_a \sin \psi \cos \theta, \quad (17)$$

where ψ and θ are the yaw and pitch angles, respectively. Since we have (3), then:

$$V_N = \frac{V_{pitot}}{c_f} \cos \psi \cos \theta + V_{N_w}, \quad (18)$$

$$V_E = \frac{V_{pitot}}{c_f} \sin \psi \cos \theta + V_{E_w}. \quad (19)$$

The values of V_{pitot} , V_N and V_E are measurable by the Pitot tube and GPS, therefore (15), (18) and (19) were used as observation equations, while c_f , V_{N_w} and V_{E_w} are estimated states in the EKF. Note that, the Euler angles (ϕ , θ and ψ) can be measured by the IMU.

4 Extended Kalman Filter

The Extended Kalman filter estimates desired states through a feedback loop. The algorithm is divided in two stages: the state predict and the measurement update. The state predict equations are responsible for projecting in time the current state and the error covariance estimates to obtain a *first* estimate for the next step. In that stage, a dynamic model shall be given. However, there is no given model to predict the wind. Thus, the model used for that stage is constant with a Gaussian input as follows:

$$\boldsymbol{\chi}_{k+1} = \mathbf{F}\boldsymbol{\chi}_k + \boldsymbol{\nu}_k, \quad (20)$$

where $\boldsymbol{\chi}_k = [\hat{V}_{N_w k} \ \hat{V}_{E_w k} \ \hat{c}_{fk}]^T$ is the estimated state vector in the instant k ,

$$\mathbf{F} = \begin{bmatrix} 1 & 0 & 0 \\ 0 & 1 & 0 \\ 0 & 0 & 1 \end{bmatrix} \text{ and } \boldsymbol{\nu}_k \sim \mathbf{N}(0, \mathbf{Q}).$$

Given the model (20), we can update the state and covariance matrix (\mathbf{P}) as follows:

$$\boldsymbol{\chi}_{k|k-1} = \mathbf{F}\boldsymbol{\chi}_{k-1}, \quad (21)$$

$$\mathbf{P}_{k|k-1} = \mathbf{F}\mathbf{P}_{k-1}\mathbf{F}^T + \mathbf{Q}. \quad (22)$$

The measurement update equations are responsible for incorporating the new measures to the *first* resulting in a *final* estimate better than the *first* one. For the accomplishment of this stage we define $\mathbf{z}_k =$

$[V_{pitot}^2 \ V_N \ V_E]^T$, $\mathbf{h}(\boldsymbol{\chi}_k) = [(15), (18), (19)]^T$ and $\mathbf{H}_k = \begin{bmatrix} \frac{\partial \mathbf{h}(\boldsymbol{\chi}_k)}{\partial V_{N_w}}, \frac{\partial \mathbf{h}(\boldsymbol{\chi}_k)}{\partial V_{E_w}}, \frac{\partial \mathbf{h}(\boldsymbol{\chi}_k)}{\partial c_f} \end{bmatrix}$, where:

$$\frac{\partial \mathbf{h}(\boldsymbol{\chi})}{\partial V_{N_w}} = [-2\hat{c}_f^2 \hat{V}_{N_w} (V_N - \hat{V}_{N_w}) \ 1 \ 0]^T,$$

$$\frac{\partial \mathbf{h}(\boldsymbol{\chi})}{\partial V_{E_w}} = [-2\hat{c}_f^2 \hat{V}_{E_w} (V_E - \hat{V}_{E_w}) \ 0 \ 1]^T \text{ and}$$

$$\frac{\partial \mathbf{h}(\boldsymbol{\chi})}{\partial c_f} = \begin{bmatrix} 2\hat{c}_f ((V_N - \hat{V}_{N_w})^2 + (V_E - \hat{V}_{E_w})^2 + (V_D)^2) \\ -\frac{V_{pitot}}{\hat{c}_f^2} \cos \psi \cos \theta \\ -\frac{V_{pitot}}{\hat{c}_f^2} \sin \psi \cos \theta \end{bmatrix}.$$

Finally, the standard algorithm of EKF can be applied as follows:

$$\tilde{\mathbf{y}}_k = \mathbf{z}_k - \mathbf{h}(\boldsymbol{\chi}_{k|k-1}),$$

$$\mathbf{C}_k = \mathbf{H}_k \mathbf{P}_{k|k-1} \mathbf{H}_k^T + \mathbf{R},$$

$$\mathbf{K}_k = \mathbf{P}_{k|k-1} \mathbf{H}_k^T \mathbf{C}_k^{-1},$$

$$\boldsymbol{\chi}_k = \boldsymbol{\chi}_{k|k-1} + \mathbf{K}_k \tilde{\mathbf{y}}_k,$$

$$\mathbf{P}_k = (\mathbf{I} - \mathbf{K}_k \mathbf{H}_k) \mathbf{P}_{k|k-1},$$

where \mathbf{P} is the covariance matrix, \mathbf{C} is the covariance error, $\tilde{\mathbf{y}}$ is the measurement error, \mathbf{K} is the Kalman gain and \mathbf{I} is the identity matrix with appropriate dimensions.

5 Neural Network

The implemented neural network (NN) is a three-layer fitting NN, which has three nonlinear hidden layers containing 24 neurons each and three linear outputs. The activation function of the nonlinear neurons are sigmoidal. The most important equations to choose the NN inputs are (15), (18) and (19). However, some of the measured values like Euler angles and velocities have nonlinearities attached to them. Therefore the input vector \mathbf{z}_{nn} and output vector $\boldsymbol{\chi}_{nn}$ of the neural network are given by:

$$\mathbf{z}_{nn} = \begin{bmatrix} V_{pitot}^2 \\ V_D^2 \\ V_N \\ V_E \\ V_E^2 \\ V_N^2 \\ V_{pitot} \cos \psi \cos \theta \\ V_{pitot} \sin \psi \cos \theta \end{bmatrix}, \quad \boldsymbol{\chi}_{nn} = \begin{bmatrix} V_{N_w} \\ V_{E_w} \\ c_f \end{bmatrix}. \quad (23)$$

It is important to note that all these values are computed with measures given by the GPS, IMU and Pitot tube sensors. The Neural network was designed in the Neural Network ToolboxTM from MATLAB. The resulting flow chart is shown in Figure 4. The dataset and method used for the training is explained in Sect. 7.

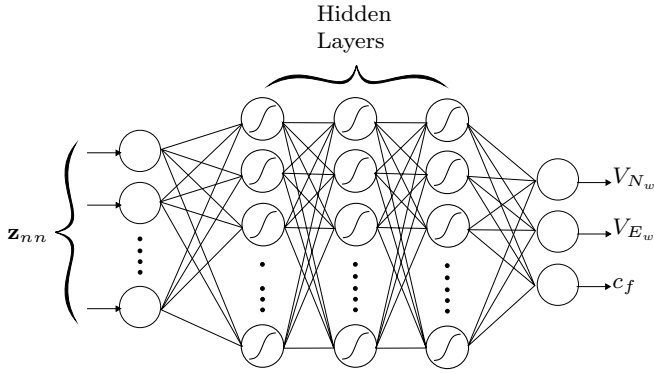


Fig. 4 Neural Network flow chart.

6 Hybrid estimator

Here we propose a hybrid estimator that performs a fusion between both estimators, namely: from the EKF designed in Sect. 4 and NN designed in Sect. 5. This fusion is performed by changing the measure update stage of the EKF approach. The NN output χ_{nn} is added to the measurement vector of the EKF as a redundant measure. Thus, resulting in the new measurement vector \mathbf{z}_{h_k} , updating function $\mathbf{h}_{h_k}(\chi_k)$ and its respective Jacobian \mathbf{H}_{h_k} shown below:

$$\mathbf{z}_{h_k} = \begin{bmatrix} \mathbf{z}_k \\ \chi_{nn} \end{bmatrix}, \mathbf{h}_{h_k}(\chi_k) = \begin{bmatrix} \mathbf{h}(\chi_k) \\ \chi_k \end{bmatrix} \text{ and } \mathbf{H}_{h_k} = \begin{bmatrix} \mathbf{H} \\ \mathbf{I}_3 \end{bmatrix},$$

where \mathbf{I}_3 is the identity matrix of third order. Then the EKF standard algorithm is used by updating the dimensions of the matrices \mathbf{C}_k , \mathbf{K}_k and \mathbf{R} . The resulting estimator has a cascaded form as illustrated in Figure 5.

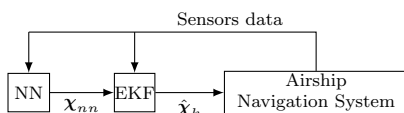


Fig. 5 Hybrid estimator with cascaded form.

It is important to highlight that the NN used here is the same NN designed in Sect. 5 and trained in Sect. 7.

7 Neural Network Training Dataset

The training dataset is composed by simulations in 16 scenarios subject to 81 different wind conditions. In all scenarios the airship is well controlled with ideal feedback. The dataset also consider sensor noise. In all situations the airship performs a typical cruise flight at 7m/s groundspeed. For each scenario were performed

simulations with wind speed at $|\mathbf{V}_w| = \{0, 1, 2, 3, 4, 5\}$ m/s and heading $\phi_w = \{0, 22.5, 45, 67.5, 90, 112.5, 135, 157.5, 180, 202.5, 225, 247.5, 270, 292.5, 315, 337.5\}$ degrees, where $\phi_w = \tan^{-1}(\frac{V_{Ew}}{V_{Nw}})$. The airship starts from origin and the paths are given by rotations of $\{0, 45, 90, 135, 180, 225, 270, 315\}$ degrees around the origin of the paths given in Figure 6. Hence, a total of 1281 simulations were performed.

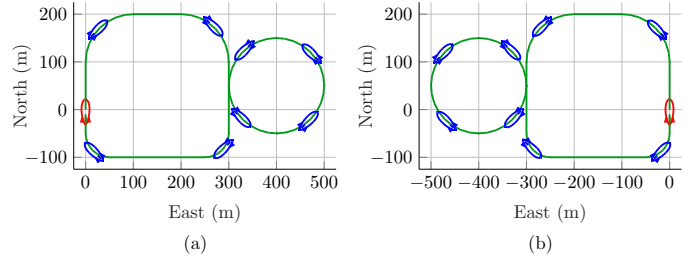


Fig. 6 Training missions: (a) first path and (b) second path.

These scenarios includes curves and straight lines in different directions assuring many different situations for the training task. The learning algorithm used for this work was Levenberg-Marquardt.

8 Simulation results

In this section, a different scenario was considered in order to validate the designed estimators. Initially the wind has absolute value $|\mathbf{V}_w| = 2m/s$ and heading $\psi_w = \frac{\pi}{2}$ rad, then in the instant $t = 160s$ the wind is intensified to $|\mathbf{V}_w| = 3m/s$ and its heading is changed to $\psi_w = \pi$. During simulation the airship is well controlled with ideal feedback, while the estimators evaluated are receiving noisy and biased data from the modelled sensors.

The simulation trajectory is shown in Figure 7. Also in this figure, five instants are highlighted with gray background in order to establish further comparisons with the results in Figure 8. Also, the results using the estimator proposed by [3] was introduced as ‘‘Cho2011’’ in order to establish a comparison. The covariance matrices used in the Model-based approaches can be found in Appendix.

It is possible to note that, the ‘‘Cho2011’’ estimator has to acquire information about the motion in all directions before it converges to the correct values. After the instant (I), all estimators converges to values within of an acceptable error. It is important to note that, the NN has some instantly variations at the trajectory curves, which deteriorate the performance. When the airship is following a straight line the designed NN has a good estimation, however biased from the real value.

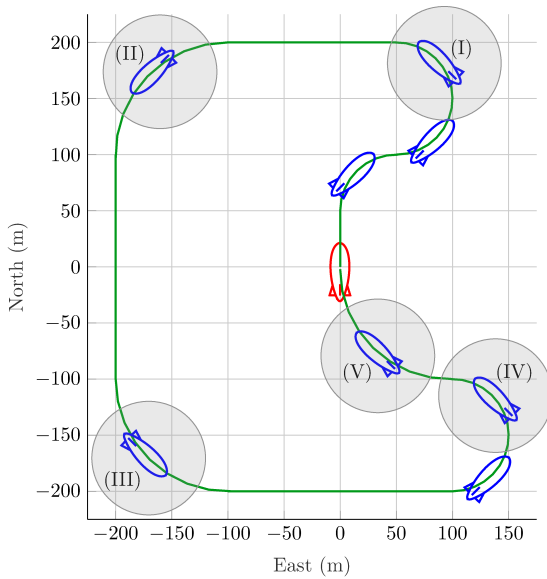


Fig. 7 Simulation trajectory.

Also in Figure 8, we can note that when the wind velocity has a significant variation just before the instant (III), the two Model-based approaches (“EKF” and “Cho2011”) do not converge immediately because both depend on information (given by the Pitot tube) about the other directions to converge to the correct wind velocity. Meanwhile the NN clearly has an instantly reaction to these variations. Even though the NN converges for a biased value, such information was sufficient to correct the estimation of the Hybrid approach before the instants (IV) and (V). In these final instants, the Model-based estimators finally converges for values within a range of acceptable error.

In Table 1 are shown the RMS values of the estimation errors $\tilde{V}_{N_w} = \hat{V}_{N_w} - V_{N_w}$ and $\tilde{V}_{E_w} = \hat{V}_{E_w} - V_{E_w}$. By the RMS values we can observe that the NN had a better estimation of V_{E_w} in comparison to the Model-based approaches. However, for the component V_{N_w} , the Model-based approaches presented a better performance. Meanwhile the “Hybrid” which has the information of both approaches had the best performance in the estimation of V_{E_w} and acceptable estimation in the V_{N_w} component.

Table 1 RMS value of the estimation error.

	\tilde{V}_{N_w} (m/s)	\tilde{V}_{E_w} (m/s)
EKF	0.58	1.42
NN	1.35	1.27
Cho2011	1.01	1.74
Hybrid	0.74	0.76

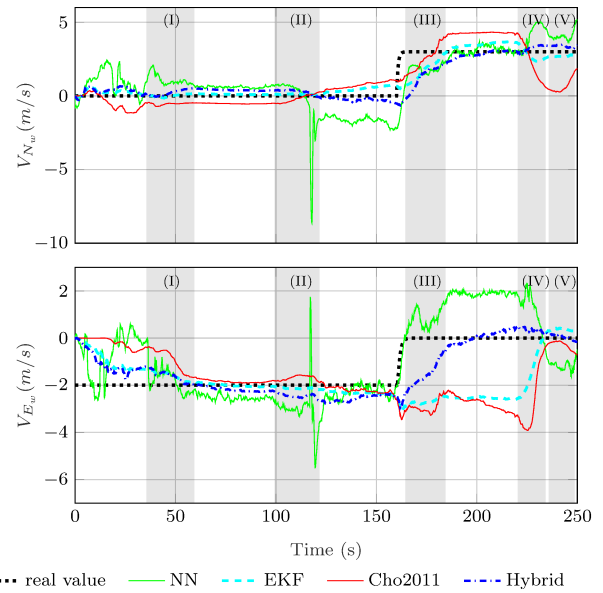


Fig. 8 Simulation in the airship nonlinear model with realistic sensor noise: wind velocity estimation in North-East frame.

9 Conclusions

In this paper we presented Model-based and Data-driven approaches for estimation of wind velocity for a robotic airship. The Model-based approach uses only kinematic equations of motion of the airship for the design of an EKF. The Data-driven proposed approach is composed by a NN trained with a big data set with several simulations in different conditions. Also, a novel Hybrid approach is proposed, by performing a fusion between the Model-based approach and the designed Data-driven approach with a cascaded structure.

The simulation results obtained showed that the proposed EKF has a slightly better performance in comparison to proposed strategies found in the literature. It occurs because of the two additional measurement update equations that we proposed. Meanwhile, the NN presented better sensibility to wind variations, however with biased estimations. As a consequence the Hybrid approach had the better performance, once it has the information of both approaches. These results show that the cooperation between both approaches (Model-based and Data-driven) can be highly effective for solving estimation problems. Future efforts will be made to validate these results outside of a simulation environment.

Appendix

The covariance matrices used for each Model-based approach are shown below:

Cho2011 :

$$\mathbf{R} = [163.84],$$

$$\mathbf{Q} = \text{diag}([10^{-3} \ 10^{-4} \ 5 \cdot 10^{-6}]).$$

EKF :

$$\mathbf{R} = \text{diag}([40.96 \ 40.96 \ 40.96]),$$

$$\mathbf{Q} = \text{diag}([10^{-4} \ 10^{-4} \ 5 \cdot 10^{-7}]).$$

Hybrid :

$$\mathbf{R} = \text{diag}([10.24 \ 10.24 \ 10.24 \ 10.24 \ 10.24 \ 10.24]),$$

$$\mathbf{Q} = \text{diag}([10^{-4} \ 10^{-4} \ 5 \cdot 10^{-7}]).$$

Acknowledgements The present work was sponsored by the Brazilian agencies CNPq and FAPESP, through Projects DRONI (CNPq 402112/2013-0), INCT-SAC (CNPq 465755/2014-3; FAPESP 2014/50851-0) and scholarships (CNPq 305600/2017-6; FAPESP BEP 2017/11423-0). Also, this work was supported by Fundação para a Ciência e a Tecnologia (FCT), through IDMEC, under LAETA, project UID/EMS/50022/2013 (Portugal). Moreover, the authors are grateful to Erasmus Mundus SMART² for the financial support through project reference 552042-EM-1-2014-1-FR-ERA MUNDUS-EMA2. Furthermore, the authors appreciate all the support given by members of the Advanced Computing, Control & Embedded Systems Laboratory (ACCES-Lab) and Laboratory of Study in Exterior Vehicles (LEVE) from University of Campinas.

References

- Allison, S., Bai, H., Jayaraman, B.: Estimating wind velocity with a neural network using quadcopter trajectories. In: AIAA Scitech 2019 Forum. American Institute of Aeronautics and Astronautics (2019)
- Chaturvedi, D.K., Chauhan, R., Kalra, P.K.: Application of generalised neural network for aircraft landing control system. *Soft Computing - A Fusion of Foundations, Methodologies and Applications* **6**(6), 441–448 (2002)
- Cho, A., Kim, J., Lee, S., Kee, C.: Wind estimation and airspeed calibration using a UAV with a single-antenna GPS receiver and pitot tube. *IEEE Transactions on Aerospace and Electronic Systems* **47**(1), 109–117 (2011)
- Elfes, A., Bueno, S.S., Ramos, J.J.G., de Paiva, E.C., Bergerman, M., Carvalho, J.R.H., Maeta, S.M., Mirisola, L.G.B., Faria, B.G., Azinheira, J.R.: Modelling, control and perception for an autonomous robotic airship. In: *Sensor Based Intelligent Robots*, pp. 216–244. Springer Science Business Media (2002)
- Johansen, T.A., Cristofaro, A., Sorensen, K., Hansen, J.M., Fossen, T.I.: On estimation of wind velocity, angle-of-attack and sideslip angle of small UAVs using standard sensors. In: 2015 International Conference on Unmanned Aircraft Systems (ICUAS). Institute of Electrical & Electronics Engineers (IEEE) (2015)
- Moutinho, A., Azinheira, J.R., de Paiva, E.C., Bueno, S.S.: Airship robust path-tracking: A tutorial on airship modelling and gain-scheduling control design. *Control Engineering Practice* **50**, 22–36 (2016)
- Perry, J., Mohamed, A., Johnson, B., Lind, R.: Estimating angle of attack and sideslip under high dynamics on small uavs. In: Proceedings of the 21st International Technical Meeting of the Satellite Division of The Institute of Navigation (ION GNSS 2008), pp. 1165–1173. Institute of Electrical and Electronics Engineers (IEEE) (2008)
- Rhudy, M.B., Gu, Y., Gross, J.N., Chao, H.: Onboard wind velocity estimation comparison for unmanned aircraft systems. *IEEE Transactions on Aerospace and Electronic Systems* **53**(1), 55–66 (2017)
- Rueda, M., Mirisola, L., Nogueira, L., Fonseca, G., Ramos, J., Koyama, M., Azinheira, J., Carvalho, R., Bueno, S., de Paiva, E.: Uma infraestrutura, de hardware, software e comunicação para a robotização de plataformas rádio - controladas: Aplicação a um dirigível robótico. In: 2017 SBAI - XIII Simpósio Brasileiro de Automação Inteligente (2017)
- Samy, I., Postlethwaite, I., Gu, D.W., Green, J.: Neural-network-based flush air data sensing system demonstrated on a mini air vehicle. *Journal of Aircraft* **47**(1), 18–31 (2010)
- Shen, S., Liu, L., Huang, B., Lin, X., Lan, W., Jin, H.: Wind speed estimation and station-keeping control for stratospheric airships with extended kalman filter. In: Proceedings of the 2015 Chinese Intelligent Automation Conference, pp. 145–157. Springer Science Business Media (2015)